The MEKaP Project: Measuring Tropospheric Impairments at Ka Band with MEO Satellites

L. Luini[1], C. Riva[1], A. Panzeri[1], A. Rocha[2], S. Mota[2], F. Marzano[3], A. Marziani[3], M. Biscarini[3], F. Consalvi[4], V. Schena[5], A. Martellucci[6]

[1]Politecnico di Milano, Milan, Italy, lorenzo.luini@polimi.it
[2]Universidade de Aveiro, Aveiro, Portugal, arocha@ua.pt
[3]Università La Sapienza, Rome, Italy, frank.marzano@uniroma1.it
[4]Fondazione Ugo Bordoni, Rome, Italy, fconsalvi@fub.it
[5]Thales Alenia Space−Italy, Rome, Italy, vincenzo.schena@thalesaleniaspace.com
[5]ESA−ESTEC, Noordwijk, The Netherlands, antonio.martellucci@esa.int

***Abstract*— The design phase of an ESA project (MEKaP – MEO Ka-band Propagation) is described. The study, involving Politecnico di Milano, Sapienza Università di Roma, Instituto de Telecomunicações-Aveiro Pole and Thales Alenia Space-Italia, aims at characterizing the main properties of the atmospheric radio channel of a MEO Ka-band SatCom system. The propagation campaign, lasting at least two years and including four ground receivers, will rely on the MEO O3b Ka-band satellite constellation, which has key characteristics for propagation measurements, such as continuous observation time (at least one satellite is always visible) and global coverage up to mid-latitudes. The experimental data collected during the campaign will be used to test and improve the available propagation models for non-geostationary systems and to extend the experimental database of radio regulatory bodies such as the ITU-R.**

***Index Terms*—Electromagnetic wave propagation, experiment, measurements.**

I. INTRODUCTION

The satellite communication (SatCom) market is gradually expanding to include new services made available by satellites flying along non-geostationary orbits (non-GSO) and operating at Ka band (and above). For example, non-GSO satellites allow for a significant reduction in the latency time (with respect to GSO systems), an easier dynamic reconfiguration of the service, as well as an improved coverage area (e.g. arctic regions).

Notwithstanding these advantages, the use of the Ka band in non-GSO systems (and, in perspective, of higher frequency bands) poses a serious challenge in terms of atmospheric impairments: rain attenuation along the variable slant path (the major contributor to link budget for high availability systems) increases quickly and varies significantly, and also the other atmospheric components (gases and clouds) can greatly contribute to the atmospheric attenuation and sky noise emission in non-GSO links [1]: indeed, the wave crosses longer paths through the troposphere when the link elevation is low, which occurs for a significant portion of the contact time. In addition, along non-GSO links, also the signal scintillation (due to tropospheric turbulence) and the atmospheric depolarization [2] are higher.

All these effects contribute to the need of a large dynamic range, which has to be accurately estimated using reliable statistical prediction models (for the system design activities, link budget analysis, trade-offs and verification by system simulation) and channel assessment techniques (during operations to control the Fade Mitigation Techniques). Unfortunately, a major limitation is that all current propagation and channel models were developed for use with GSO satellites [3]; in addition, so far, all the long-term propagation campaigns and testing activities have been performed using beacon signals transmitted from GSO platforms [4]. As a result, there is an increasing interest in collecting propagation measurements along non-GSO links and in applying them for the improvement and validation of existing models, as well as for the development of new ones [5].

This contribution describes the design of an ESA project for a non-GSO Ka band propagation campaign (MEKaP – MEO Ka-band Propagation), involving Politecnico di Milano (PoliMi), Sapienza Università di Roma (SUR), Instituto de Telecomunicações-Aveiro Pole (IT-AV) and Thales Alenia Space-Italia (TAS-I). The study will use the Ka-band signal transmitted by the MEO O3b satellite constellation, which has key characteristics for the needs of long-term propagation measurements, such as continuous observation time (at least one satellite is always visible), satisfactory visibility (approximately 1.5 hours per contact time of each satellite), global coverage up to mid-latitudes. The propagation campaign, lasting at least two years and including four ground receivers, aims at characterizing the main properties of the atmospheric radio channel of a MEO Ka-band SatCom system. The experimental data collected during the campaign will be used to test and improve the available propagation models for non-GSO systems and to extend the experimental database of radio regulatory bodies such as the International Telecommunication Union – Radiocommunication Sector (ITU-R).

II. SPACE SEGMENT: THE O3B CONSTELLATION

The MEKaP experimental campaign relies on the O3b satellite constellation, which provides the first practical chance to perform studies on electromagnetic wave propagation from MEO satellites: in fact, the high number of satellites composing the fleet guarantees continuous signal coverage at latitudes between 62° N and 62° S. Table I summarizes some key features of the O3b constellation [6], while Fig. 1 shows the coverage area and the system gateways.

TABLE I. O3B CONSTELLATION MAIN FEATURES [6]

Orbit type	MEO on the Equatorial plane
Latitude coverage	± 45° (Standard service) ± 62° (Limited service)
Satellite altitude	8062 km
Satellites	21 currently operative [7]
Frequency band (including telemetry)	Ka band: 17.7−20.2 GHz
Antennas	12 (2 gateway + 10 user)
Latency	~150 ms (round trip)

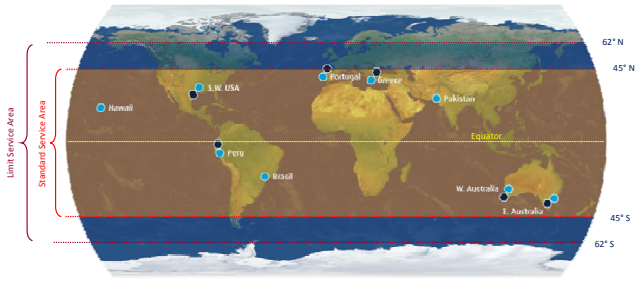

Fig. 1. O3b constellation coverage and main gateway locations.

As specified in Table I, the campaign will take advantage of the O3b satellite telemetry (TM) signals, which are transmitted at frequencies in the 17.7−20.2 GHz band.

Differently from the typical propagation experiments exploiting beacon signals emitted by GSO satellites (e.g. the Alphasat campaign [4]), the MEKaP experiment poses an additional challenge: the TM signal consists in a data stream that is phase modulated on the telemetry carrier. As explained later in Section IV.A, this calls for the definition and implementation of an ad-hoc signal acquisition algorithm to identify and correctly measure the carrier frequency.

III. GROUND SEGMENT

A. Experimental Sites

The sites selected for the installation of the receiving equipment are listed in Table II: one site is located in Portugal (Aveiro), another one in Northern Italy (Milan), while two of them are in Rome, and lie just some kilometers apart (roughly 13 km). The latter sites will allow conducting site diversity investigations.

TABLE II. GEOGRAPHICAL COORDINATES OF THE MEKAP EXPERIMENTAL SITES

Site	Milan (PoliMi)	Rome (SUR)	Rome (TAS-I)	Aveiro (IT-AV)
Country	Italy	Italy	Italy	Portugal
Latitude	45° 29′ N	41° 53’ N	41° 58’ N	40°37′ N
Longitude	9° 14′ E	12° 29’ E	12° 36’ E	8°40′ W
Altitude	120 m	21 m	21 m	18 m

The visibility of O3b satellites from the experimental sites was investigated by means of the commercial software STK (System Tool Kit). The analysis on the O3b satellite visibility has shown that:

- at least 2 satellites are always visible at the same time, but most of the time this number ranges between 3 and 4; this will allow for uninterrupted measurement of the telemetry signals;
- the maximum elevation angle of O3b satellites is: 20.2°, 24.5° and 26.1° for Milan, Rome and Aveiro, respectively;
- the link azimuth ranges approximately between 120° and 240º.

B. MEKaP Propagation terminal

In the framework of radio wave propagation campaigns, two architectures are commonly employed to measure the power of the beacon signal emitted by the satellite: phase locked (PLL) loop receivers; Fast Fourier Transform (FFT) receivers, including a Software Defined Radio (SDR) card for signal processing tasks. For the MEKaP campaign, the latter is preferred mainly because of the following advantages:

- easy implementation thanks to the processing power of current computers;
- immediate measurement recovery as soon as a faded signal rises again sufficiently above the receiver noise floor;
- simple estimation of the Noise Spectral Density (NSD), which, in turn, can help improve the accuracy of the measured signal.

In addition, the receiver equipment must meet the following basic requirements:

- a 10-MHz bandwidth of the last IF stage of the receiver before the SDR card, necessary to accommodate all the telemetry channels; this will also allow taking in due account the Doppler shift of the TM beacon, which has a maximum absolute value of 80 kHz (rising and setting satellite positions);
- a tracking system speed of 1°/s: although tracking velocities of 0.03°/s in azimuth and of 0.015°/s in elevation would be sufficient to track the O3b satellites, such a speed will allow a quick handover (less than 2 minutes) from a setting satellite to a rising one, thus maximizing the data availability time.

During the campaign, the receivers will track the O3b satellites, with minimum elevation angle of 10°, using as input the elevation and azimuth angles estimated by coupling

the Simplified General Perturbation model SGP4 [8] and the freely available Two-Line Element (TLE) files updated approximately on a daily basis by the North American Aerospace Defense Command (NORAD) [7].

C. Link Budget

The link budget was calculated for each experimental site to correctly dimension the receiving equipment, as well as to estimate the dynamic range available to characterize the radio channel for the worst case scenario of lower elevation angle $\theta = 10°$. To this aim, the atmospheric attenuation and the sky noise were estimated by using the propagation models recommended by ITU-R in the P-series section. In addition, the link budget must take into account a pointing loss of the on-board antenna, due to the fact that, during the pass, the satellite antenna likely points to one of the O3b gateways in the coverage area: we estimate that the antenna pointing loss is 3.7 dB in the worst case (i.e. assuming that the on-board antenna points to the farthest GW from a terminal).

Due to the limited transmit power (assumed to be 2.5 dBW on average) and the modulation loss (5.3 dB for a phase modulation with an index assumed to be of 1 radian), the maximum tropospheric fade ranges between 15 dB and 22.4 dB, using antennas with diameter between 1.2 m (IT-AV) and 2.4 m (TAS-I), a Low Noise Amplifier (LNA) with 1.5 dB noise figure and an integration bandwidth of 40 to 50 Hz around the carrier frequency.

IV. Data Collection and Analysis

A. Signal Measurement Algorithm

The signal will be acquired at least at 400 kS/s sampling rate (for both I and Q components), which will accommodate Doppler frequency variations and will allow estimating the Noise Spectral Density (NSD) with a small fluctuation.

In order to understand the detection issues, TM beacon time series were simulated with an unmodulated Carrier-to-Noise Ratio (CNR) of 50 dBHz, phase modulation index $\beta = 1$, sampling frequency f_s = 327680 S/s (I/Q), using the carrier at f_c = 81920 Hz. The spectrum was then calculated with 1 Hz resolution and is depicted in Fig. 2: it contains the carrier, with -5.3 dB power reduction with respect to the the unmodulated case, and sidebands at $\pm n \times 8192$ Hz, being n an odd number.

If the data stream is composed of randomly distributed '0's and '1's, the power of the sidebands spreads across the spectrum and the carrier appears as a narrow spectral line placed within the first two sidebands (see curves labelled as "Spec 1" and "Spec 2" in Fig. 2). If the data stream is composed only by '0's (or '1's) (i.e., no information transmitted), the sidebands become narrow spectral lines (see plot "Spec 3" in Fig. 2), with the first two lines (n = 1) having a power similar to that of the carrier (assuming a phase modulation index $\beta = 1$). Preliminary observations of the TM spectrum of a few O3b satellites using a preliminary signal detection test bed setup (see Section IV.B) seem to confirm that the signal changes frequently between the two states described above.

Signal detection will use spectral techniques, but differently from a beacon signal (single spectral line) [9], unambiguous carrier identification is of greater complexity. The detection of an unmodulated beacon is usually performed by searching the spectrum for the spectral line with the highest power and, then, the total beacon power is obtained by summing (integrating) the power of this line and of a set of other lines around it, i.e. within a bandwidth B_W (typically 40 to 50 Hz).

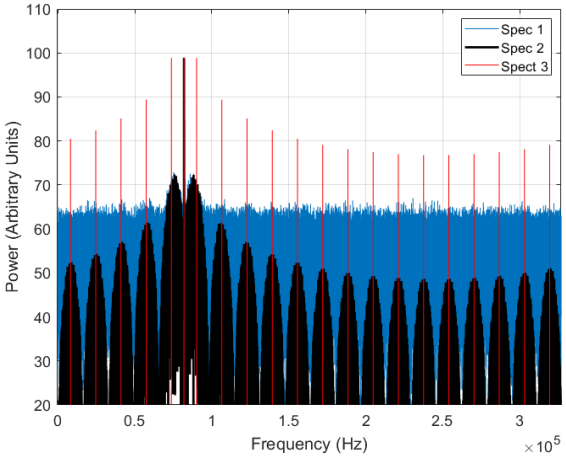

Fig. 2. TM signal simulated spectra. "Spec 1" (with AWGN noise), "Spec 2" (random distribution of '0's and '1's), "Spec 3" (no information being transmitted).

On the contrary, the O3b signal can exhibit sporadically narrow sidebands with a power similar to or greater than the carrier, which can lead, together with additive noise integrated power, to the identification of the wrong carrier. In order to make the carrier identification more robust, the procedures currently under refinement are based on the following steps:

- The spectrum is searched to find the highest power FFT spectral line, f_0: the corresponding integrated power, P_0 (within the bandwidth B_W) is calculated.
- The set of integrated power in the same bandwidth B_W, $\{P_{-n} \ldots P_{-1}\ P_{+1} \ldots P_n\}$, around the frequencies $f_0 \pm n8192$ Hz, with n = 1, 2, … is as well calculated;
- The NSD is computed by integrating the whole spectrum power (excluding the portion of the spectrum affected by the SDR filters, and the range where most of the signal power lies) and then dividing the result by the integration bandwidth.
- The Signal-to-Noise Ratio (SNR) is calculated for all the power lines $\{SNR_{-n} \ldots SNR_{-1}\ SNR_0\ SNR_{+1} \ldots SNR_n\}$.

Starting from the SNR value, an algorithm is run, which is able to identity unambiguously the carrier among the candidate pool. Then the power, frequency and NSD of the car-

rier are stored. The NSD will be used to unbias the detected carrier power and support the data processing algorithms.

The algorithm was tested with synthetic time series of the TM signal and it performs very well down to a CNR of 22 dBHz using FFTs with 4 Hz resolution.

B. *Preliminary measurements*

A set of O3B TM short duration measurements at 2 MS/s was performed in Rome with a preliminary signal test-bed using a receiver borrowed from the Alphasat campaign.

The algorithm described in Section IV.A was applied to the measured TM signal time series and it performed well (no failures) down to a CNR = 22 dBHz, thus achieving the same performance as that obtained with the simulated data described in the previous chapter. An example of the estimated carrier power is depicted in Fig. 3, with the calculated CNR ranging between 22 and 33 dBHz.

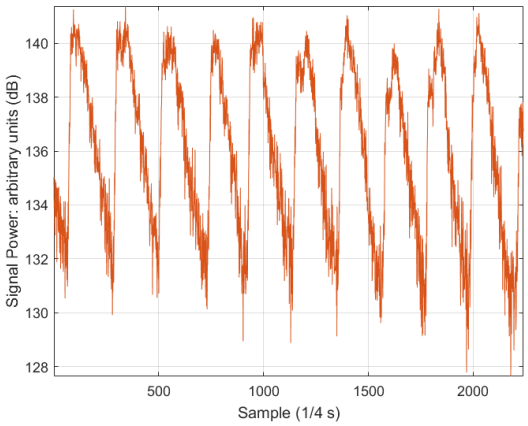

Fig. 3. Carrier power received from an O3b satellite (about 9 minutes).

The periodic triangular cycles of the signal observed in Fig. 3 are due to the large time interval for the movement of the antenna tracking system (1 step per minute): between two pointing instants, the signal amplitude decreases because the satellite moves away from the receiver antenna boresight.

C. *Data Preprocessing and Tropospheric Attenuation Extraction*

The processing of the experimental data collected during the MEKaP campaign to derive total and rain-only attenuation will be a complex problem. In fact, unlike the case of GSO satellites, the MEO satellite contact time is limited, and the elevation and azimuth change continuously: as a result, the clear sky attenuation level (i.e. only due to gases) will also change. Moreover, two consecutive satellites will be observed at very different azimuth angles and the satellite beacons will probably have slightly different EIRP levels. These are only some of the elements that will complicate the derivation of the total tropospheric attenuation A from the beacon power received on the ground, P_B.

The key point to derive the total attenuation A is to use as reference the gaseous attenuation A_G [10], which, in turn, result from the combination of the absorption due to water vapor, A_V, and to the one due to oxygen, A_{OX}. The calculation of A_G will make use of the ERA5 re-analysis data, which represent a good compromise between acceptable spatial (0.28125°×0.28125° horizontally, 137 vertical layers up to 70 km) and temporal resolution −1 hour (at least for gaseous attenuation whose temporal and spatial variability is quite limited), and improved accuracy with respect to forecast data. More specifically, full vertical profiles of the atmosphere will be used: by collecting atmospheric profiles of several NWP pixels around the ground station, the calculation of A_G can be achieved by integrating the specific attenuation along the path, i.e. by selecting the proper pixels and vertical layers crossed by the link for every elevation and azimuth position. As an example, Fig. 4 shows the ERA5 pixels crossed by the radio link (the red line represent the projection of the link on the ground) for Milan, considering a typical passage of an O3b satellite and setting the limit of the troposphere at 20 km.

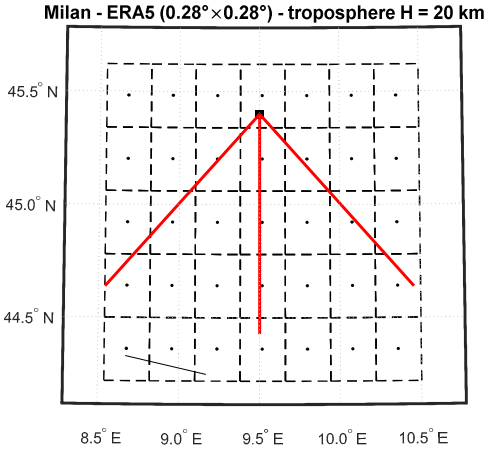

Fig. 4. ERA5 database pixels crossed by the the link to O3b satellites from Milan.

A chance to partially assess the accuracy in estimating the gaseous attenuation using ERA5 data comes from the availability of radiometric data at Politecnico di Milano. Collected at fixed elevation angle (35.4°) by a microwave radiometer (MWR) in the framework of the Alphasat propagation experiment [4], the brightness temperatures at 23.8, 31.4, 72.5 and 82.5 GHz can be used to retrieve A_V along the path, using well-established retrieval algorithms [11]; indeed, at Ka band, water vapor is the major responsible for the gaseous attenuation, and it can be calculated as [11]:

$$A_V = a_V V \tag{1}$$

In (1), a_V is the water vapor mass absorption coefficient that can be extracted from recommendation ITU-R P.676-12 (Section 2.3) [12].

Given the linear dependence between A_V and V, the comparison shown in Fig. 5 allows shedding some light on the accuracy of using ERA5 to estimate the attenuation due to gases. The figure compares V as retrieved using the MWR

(14 February 2019) and as obtained by integrating, along the same link to the Alphasat satellite, the water vapor content provided by the ERA5 database. Reported in Fig. 5 as reference are also the V values obtained from the radiosonde observations (RAOBS) launched at Linate Airport (5 km from the experimental site): the agreement between ERA5-derived results and the two other sources is satisfactory.

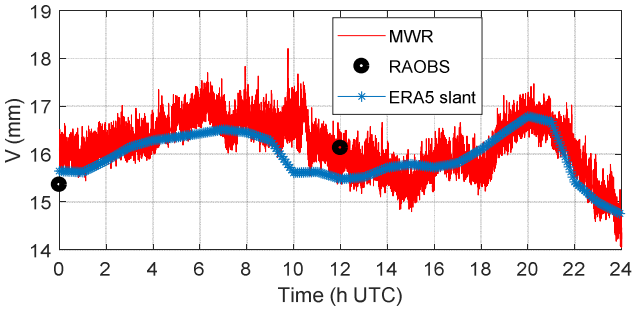

Fig. 5. Integrated water vapor content: path to the Alphasat satellite from the Milan receiving station (elevation angle of 35.4°); comparison between different sources on the 14 February 2019.

Fig. 6 extends the example reported in Fig. 5 by depicting the trend of the gaseous attenuation A_G on the 3 April 2019 (f = 19.3 GHz), affecting the link from Milan to the O3b satellites (calculated using the models in Annex 1 of [12]), whose elevation is indicated in Fig. 7: each line is associated to a different satellite of the constellation passing over the station. In this case, the handover strategy, one of the possible ones to be selected during the propagation campaign, consists in tracking a satellite until it sets and then shifting to the one with the highest elevation.

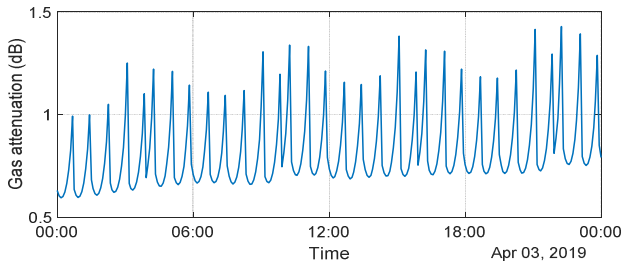

Fig. 6. Trend of the gas attenuation A_G on the 3 April 2019, affecting the link from Milan to the O3b satellites (f = 19.3 GHz).

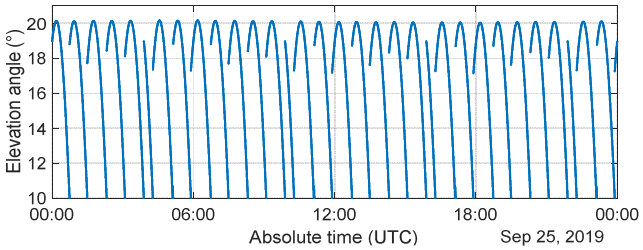

Fig. 7. Elevation of the O3b satellites on the 3 April 2019 (Milan site).

V. Conclusions

This contribution provides an overview of MEKaP (MEO Ka-band Propagation), an ESA project supported by the Portugal and Italian national delegations, which aims at characterizing the main properties of the atmospheric radio channel of a MEO Ka-band SatCom system. The design phase has been concluded and the procurement of the ground stations (which will likely be operative by February/March 2020) has started. The preliminary measurements have shown a satisfactory performance of the algorithm devised to identify the carrier and to estimate its power, starting from the received TM signal. The experimental data collected during the two-year campaign will be used to test and improve the available propagation models for non-geostationary systems and to extend the experimental database of radio regulatory bodies (e.g. ITU-R).

References

[1] C. Riva, C. Capsoni, L. Luini, M. Luccini, R. Nebuloni, A. Martellucci, "The Challenge of Using the W Band in Satellite Communication," *Int. J. Satell. Commun. Network.* 2014; 32:187–200.

[2] A. Paraboni, A. Martellucci, C. Capsoni, C. Riva, "The Physical Basis of Atmospheric Depolarization in Slant Paths in the V Band: Theory, Italsat Experiment and Models," *IEEE Transactions on Antennas and Propagation*, Vol. 59, No 11, pp. 4301 - 4314, 2011.

[3] Recommendation ITU-R P.618-13, "Propagation data and prediction methods required for the design of Earth-space telecommunication systems," Geneva, 2017.

[4] M. Zemba, J. Nessel, L. Luini, C. Riva, "Three Years of Atmospheric Characterization at Ka/Q-band with the NASA/POLIMI Alphasat Receiver in Milan, Italy." *EuCAP 2018*, 9-13 April 2018, pp. 1-5, London, UK.

[5] N. Jeannin, et al., "Atmospheric channel simulator for the simulation of propagation impairments for Ka band data downlink", *EuCAP 2014*, 6-11 April 2014, p. 3357–3361, The Haugue, The Netherlands.

[6] "O3b – A different approach to Ka-band satellite system design and spectrum sharing", available online at https://www.itu.int/dms_pub/itu-r/md/12/iturka.band/c/R12-ITURKA.BAND-C-0010!!PDF-E.pdf

[7] https://celestrak.com/NORAD/elements/. October 2019.

[8] D. A. Vallado, P. Crawford, R. Hujsak, T. S. Kelso, (August 2006) "Revisiting Spacetrack Report #3," *AIAA/AAS Astrodynamics Specialist Conference*, AIAA 2006-6753, Keystone, Colorado, August 21-24, 2006.

[9] A. Rocha, T. Pereira, S. Mota, and F. Jorge, "Alphasat experiment at Aveiro," in *2016 10th European Conference on Antennas and Propagation (EuCAP)*, 2016, pp. 1–5.

[10] L. Luini, C. Riva, R. Nebuloni, M. Mauri, J. Nessel, A. Fanti, "Calibration and Use of Microwave Radiometers in Multiple-site EM Wave Propagation Experiments", *EuCAP 2018*, 9-13 April 2018, pp. 1-5, London, UK.

[11] L. Luini, C. Riva, C. Capsoni, A. Martellucci, "Attenuation in non rainy conditions at millimeter wavelengths: assessment of a procedure", *IEEE Transactions on Geoscience and Remote Sensing*, pp. 2150-2157, Vol. 45, Issue 7, July 2007.

[12] Recommendation ITU-R P.676-12, "Attenuation by atmospheric gases and related effects," Geneva, 2019.